



CONTROL OF HUMAN ATRIAL FIBRILLATION

W. L. DITTO*, M. L. SPANO[†], V. IN*[†], J. NEFF* and B. MEADOWS*
*Applied Chaos Laboratory, GT/Emory Biomedical Engineering Department,
Georgia Institute of Technology, Atlanta, GA 30332-0535, USA*

**Control Dynamics Inc., 1662 101st Place SE, Bellevue, WA 98004, USA*

*[†]Naval Surface Warfare Center, Carderock Laboratory,
Code 684, W. Bethesda, MD 20817, USA*

J. J. LANGBERG, A. BOLMANN and K. McTEAGUE
Electrophysiology Laboratory, Emory University Hospital, Atlanta, GA 30322, USA

Received February 17, 1999; Revised September 10, 1999

Chaos control has been applied to control atrial fibrillation in humans. Results are presented on the application and evaluation of chaos control for slowing and regularizing local electrical activation of the right atrium of humans during induced atrial fibrillation.

1. Introduction

Atrial fibrillation is the most common arrhythmia requiring treatment intervention. [Prystowsky *et al.*, 1996]. The prevalence of atrial fibrillation increases with age, occurring in more than 5% of the population over the age of 65 [Kannel *et al.*, 1982]. During atrial fibrillation the rapid and irregular ventricular rate as well as the loss of atrial mechanical function diminish overall cardiac performance and may cause palpitation, breathlessness, fatigue and lightheadedness. In addition to these disabilities, atrial fibrillation dramatically increases the risk of stroke and cardiovascular-related death [Kannel *et al.*, 1982].

Normally, electrical activation of the heart is initiated by the sinus node and propagates through the atrium as a single activation wavefront. Atrial fibrillation occurs when this orderly wavefront fragments into multiple components that spread in an irregular, rapidly and continuously changing pattern.

Evidence has suggested that biological activity, including the beating of myocytes *in vitro* [Chialvo *et al.*, 1990; Chialvo, 1990], cardiac arrhythmias [Garfinkel *et al.*, 1992; Hall *et al.*, 1997], human

atrial fibrillation [Garfinkel *et al.*, 1997], and brain hippocampal electrical bursting [Schiff *et al.*, 1994] exhibit deterministic dynamical behavior comparable to the chaotic instabilities found in other nonlinear systems [So *et al.*, 1996, 1997; Shinbrot *et al.*, 1993; Witkowski *et al.*, 1995]. Chaos is the agglomeration of a large number of unstable periodic motions. Such unstable behavior with its associated local dynamics forms the basis for various chaos control techniques [Shinbrot *et al.*, 1993; Ditto & Pecora, 1993; Ott & Spano, 1995; Christini & Collins, 1995, 1996; Pei & Moss, 1996]. Recent work on the control of chaos in low-dimensional [Shinbrot *et al.*, 1993; Ditto & Pecora, 1993; Ott & Spano, 1995], high-dimensional [Ding *et al.*, 1996], and spatially extended chaos [Petrov *et al.*, 1996; Petrov & Showalter, 1996] in physical and biological systems has enabled the application of chaos control to human atrial fibrillation.

2. Experimental Details

This chaos control study was performed on 25 patients undergoing clinically-indicated electrophysiological testing. The study was conducted under a protocol approved by the Human Research

Committee at Emory University and all patients gave written, informed consent. A quadripolar electrode catheter with 5 mm interelectrode spacing was inserted via the femoral vein and advanced under fluoroscopic guidance to the anterolateral aspect of the right atrium as shown in Fig. 1. The tip of the catheter was positioned to achieve a bipolar stimulation threshold of ≤ 2 mA at a 2 ms pulse width. Atrial fibrillation was induced using rapid pacing (50 Hz) for 1 to 2 seconds. Local atrial activation was recorded from the proximal pair of electrodes (poles 3 and 4). The signal was amplified (with no filtering) and sent to the active control and passive recording computers where it was digitized at 2 kHz and 5 kHz, respectively. For detection of atrial activation we maintained a running background, which consisted of an average of the previous 6000 points (3 seconds) of the signal (minus a small region around each previously de-

tected activation). An activation was determined to have occurred if the signal increased through a threshold (a multiple of the standard deviation of the width of the running background), passed over a local maximum and then decreased through another threshold (again a multiple of the standard deviation of the running background) that was lower than the first threshold. The activation time was then calculated as the time at which the signal reached half the height of the rising edge of the local maximum. The rising edge was chosen since it is possible to determine the time at which it occurs with greater precision than one can determine the activation peak time, especially in the presence of experimental noise. This technique was accurate, in concordance with the timing of automatic detection and subsequent manual analysis in 90–97% of the intervals, depending on the signal quality. Stimulus artifact rejection was accomplished in software

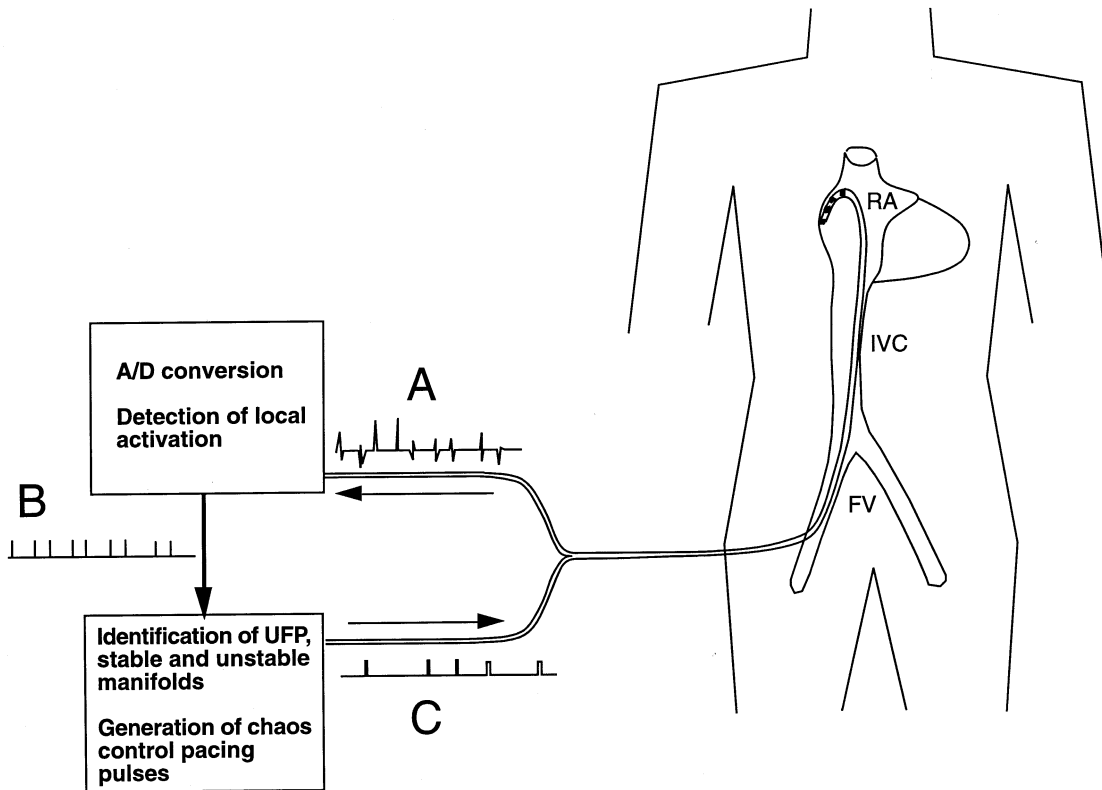


Fig. 1. Summary of the experimental design. A quadripolar electrode catheter was inserted in the femoral vein (FV), advanced through the inferior vena cava (IVC) and positioned in the lateral right atrium (RA). During atrial fibrillation, electrograms (A) recorded from the proximal pair of electrodes were amplified, digitized and local activations automatically detected. This timing information (B) was used to characterize the chaotic dynamics of the system with identification of the unstable fixed point (UFP), as well as the stable and unstable manifolds. The control algorithm then generated pacing pulses (C) at times predicted to move the system towards a stable (periodic) state.

by blanking the signal for 5 to 10 ms after applying a stimulus. We then monitored the signal for an activation in response to the stimulus for the subsequent 50 ms. If no such activation was observed, we assumed an activation had occurred within the stimulus blanking period and took the stimulus time as the activation time. Control stimuli were output from the computer and used to trigger a stimulus isolation unit that was connected to the distal poles (1 and 2) of the atrial electrode catheter.

All activations from the control runs were reviewed and verified by both manual and computer detection of events in endocardial electrograms during each intervention using the recordings from the backup recording computer.

3. Chaos Control

Chaos control consists of: (1) constructing a Poincaré plot consisting of intervals, I_n , between the current activation and the previous activation plotted against the previous intervals, I_{n-1} ; (2) a learning phase where we identified and characterized unstable fixed points on the Poincaré plot; and (3) an intervention phase consisting of precisely-timed stimuli designed to place the next Poincaré plot point onto the unstable manifold of the identified fixed point. Thus each control attempt consisted of a learning phase and a control phase. During the learning phase an unstable fixed point (UFP) was identified [Garfinkel *et al.*, 1992; Schiff *et al.*, 1994] and characterized in real time [Pierson

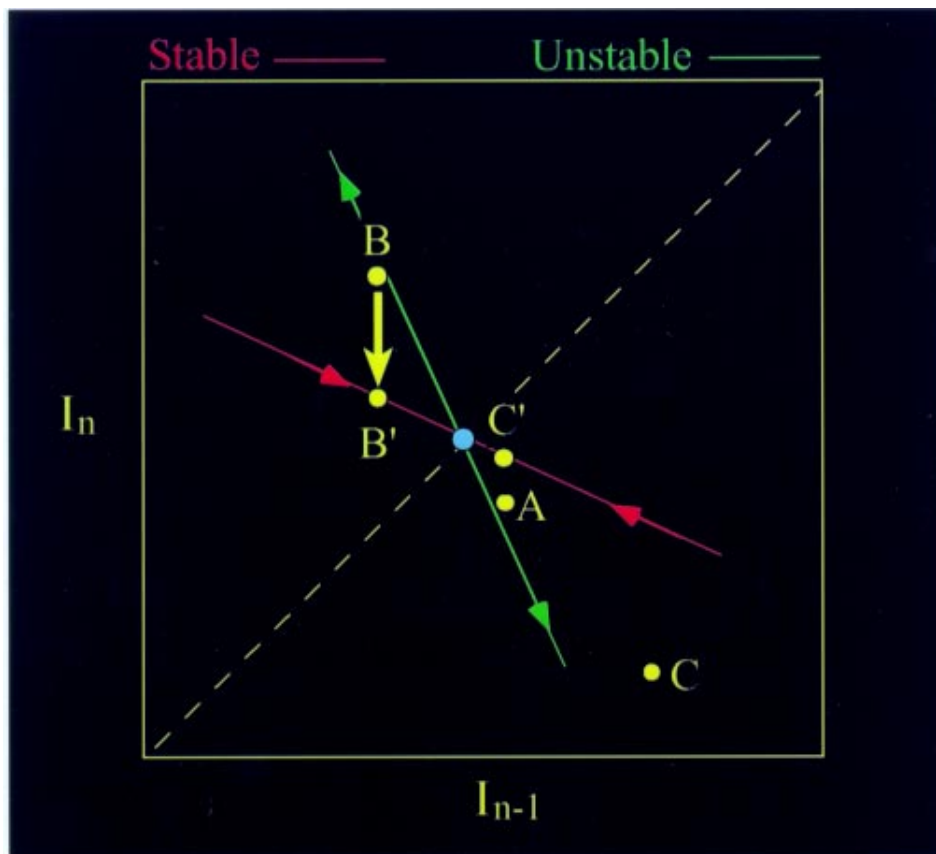


Fig. 2. Schematic of chaos control technique. I_n is the current interval between beats and I_{n-1} is the previous interval between beats. The central dot represents an unstable fixed point. The stable (inward arrows) and unstable (outward arrows) manifolds are shown as calculated from a close return to the unstable fixed point from the learning phase of the algorithm. With no intervention, the natural dynamics around the unstable fixed point carries the activation intervals from A to B to C as stretched out along the unstable direction. Chaos control is implemented after a determination of the stable and unstable directions around a located unstable fixed point. An interval landing at A is predicted to land at B from the local dynamics. A stimulus is introduced into the human high right atrium to force a premature beat that will direct A to B' instead of B. Then the local contraction along the stable direction pulls the next interval closer (to C') to the unstable fixed point. Thus the sequence of ABC is modified to AB'C'. This process is repeated in a feedback loop to stabilize the unstable fixed point.

& Moss, 1995]. A schematic of the process is presented in Fig. 2. Further details of the process may be found in [Garfinkel *et al.*, 1993; Schiff *et al.*, 1995]. Note that this technique depends on the presence of a single UPO and not necessarily on the presence of full-blown chaos, although the algorithm was initially developed for use in chaos control. Whether one concludes that this system is indeed “chaotic,” the presence of the UPO makes chaos control techniques appropriate.

Additionally, to demonstrate that we were indeed attempting control around an unstable fixed point rather than a noisy random point, we applied the algorithm of So *et al.* [1996, 1997] (after the control runs since this method is too computationally costly to implement in real time) to determine whether it also detected the fixed point around which we had attempted control. The So algorithm transforms the data such that in a suitable phase space, points “near” an unstable fixed

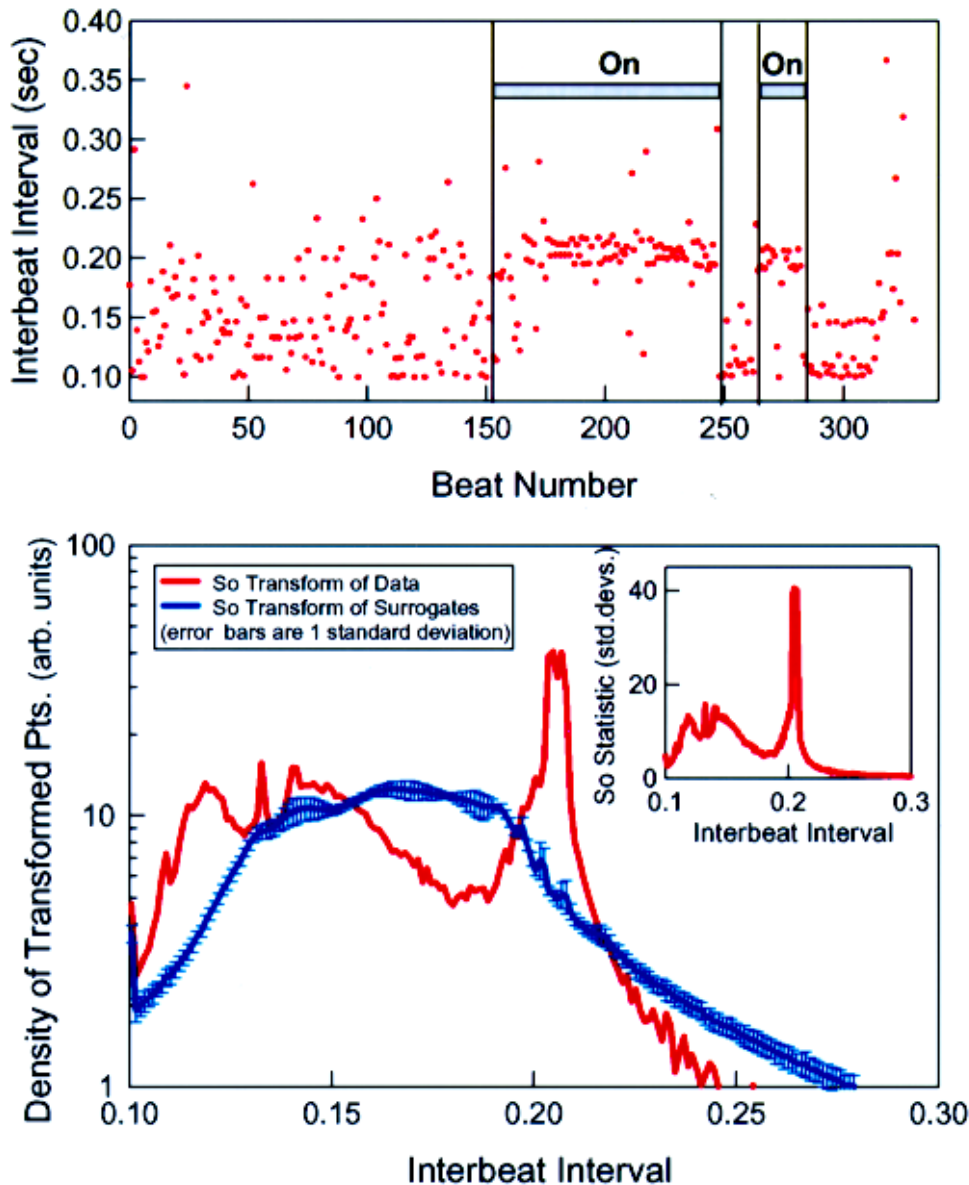


Fig. 3. (a) Time series of a typical control run. The bars indicate times when chaos control was active. Times prior to beat 150 comprise the learning period. (b) The So transform of this data (red). The solid blue line indicates the average of 100 surrogates, with error bars denoting the standard deviation at each point. (Inset) So statistic (as described in the text).

point are mapped onto the unstable fixed point position. Other points are mapped randomly over the attractor. Thus, in a 1D histogram of the distribution of the transformed points, UPO's are observable as sharp peaks. In this case "near" refers to a region around the UPO that can be approximated by a linear map. (Higher-order versions of this method have also been formulated.) This linear region is similar to the linear region used by Pierson *et al.* [1995].

Typical results are presented in Fig. 3(a). For this same data the *So transform* is shown in Fig. 3(b). Note the strong peak in the transform is just above an interval value of 0.2 s, which is identical to the interval around which the control was implemented.

After applying the *So transform* to our data, we then applied it to 100 randomly shuffled surrogates ([Theiler *et al.*, 1992], please note that Theiler in this reference recommends first the use of randomly shuffled surrogates as a null hypothesis. Other surrogates should be used only if these surrogates are inadequate. In this case the usual alternative surrogate, the Gaussian scaled, phase randomized surrogate, is not acceptable here *since it preserves short range correlations*, the very item that we are trying to detect in the data). We then computed the *So statistic*, which is the transformed data minus the average of the transforms of the surrogate data sets, and divided by the standard deviation of the transformed surrogate data sets on a point by point basis. (This differs slightly from the procedure outlined in [So *et al.*, 1996].) The inset of Fig. 3 shows this statistic, which is over 40 standard deviations above the surrogate background.

Thus we have strong corroborating statistical evidence for the existence of the UFP's about which we were controlling. All successful control runs had similar statistics.

After the identification and characterization of the UFP the computer waited until a close approach to the UFP was detected ($|I_n - I_{n-1}| < \varepsilon$ where ε defines the control region and is a fraction of the total attractor size). The algorithm then initiated a control stimulus that moved the next point on the Poincaré plot (as predicted by the local dynamics of the UFP) onto the stable manifold (i.e. the contracting direction) of the UFP, thereby allowing the natural dynamics of the system to subsequently draw the system state onto the UFP itself. Stimuli were administered on subsequent points to keep the system on the stable manifold. Thus the system

state was continually contracted towards the UFP. If the current point on the Poincaré plot strayed outside the control region, stimuli were then discontinued until the system state point re-entered the control region. At this time control stimuli were reinitiated using the same dynamical constants measured in the earlier learning phase. No additional learning was used.

4. Human Chaos Control Results

The outcome of chaos control was categorized as follows: (1) *Excellent Chaos Control* was defined by successful capture (a capture is an activation within 15 ms of the application of a control stimulus) for at least 25 sequential intervals around a UFP. The mean of the controlled intervals was equal to or longer than the mean of the activation intervals of the spontaneous atrial fibrillation and the standard deviation from the mean was at least two times less than the standard deviation from the mean of the uncontrolled activation intervals as shown in Fig. 4(a). However, since this algorithm is implemented in a 2D Poincaré section, it is necessary to consider the results on that section. These are displayed in Figs. 4(b) and 4(c). Figure 4(b) shows the distribution of the data before control was implemented for a typical case, while Fig. 4(c) gives the distribution as a result of the control algorithm. The symmetry is important because it indicates that the deviations around the control point are truly random and not the result of poor control technique or bad control parameters. (2) *Partial Chaos Control* was defined as in (1) except with more frequent losses of control (10–50% of total intervals during chaos control were escapes from the control region) about the UFP. (3) *Unsuccessful Chaos Control* was defined as all other cases, including those with infrequent capture, lack of suitable UFP's, indiscernible dynamics about the UFP, and all other results. Out of the 25 patients in the study, excellent chaos control was achieved in 9 patients (36%), partial chaos control was achieved in 10 patients (40%) and unsuccessful chaos control was seen in the remaining 6 patients (24%). More than 80% of the interventions that exhibited partial control had evidence of incomplete activation *detection* as the cause for the frequent loss of control, rather than any failure of the chaos control algorithm. Additional reasons for loss of control included poor characterization of UFP's and

rapid changes in the (uncontrolled) dynamics. To diagnose poor characterization of the UFP's, control was turned off and then reinitiated with a new learning phase. After the second learning phase was completed, a dramatically different UFP was found, thus calling into question the accuracy of the original UFP characterization. In contrast, during excellent chaos control we were able to discontinue chaos control and subsequently reacquire the same UFP as shown in Fig. 3(a). In these cases the UFP always had similar values for its position and its manifolds to those that were found previously. More significantly, the chaos control remained excellent. In the six unsuccessful control attempts, we were never able to both locate and control (for any sig-

nificant length of time) a UFP with a mean cycle length at or above the uncontrolled mean.

It has been demonstrated [Alessie *et al.*, 1991; Kirchoff *et al.*, 1993] that during atrial fibrillation conventional fixed-rate pacing (stimulation at a constant cycle length) and demand pacing (a stimulation rate at which the intrinsic activation interval exceeds the programmed pacing interval) only entrains local activations in a narrow window of cycle lengths around the mean activation interval. Both techniques suffer from inconsistent capture when pacing at shorter and longer cycle lengths [Alessie *et al.*, 1991; Kirchoff *et al.*, 1993]. When pacing at intervals much shorter than the mean interval, either method only eliminates the long intervals,

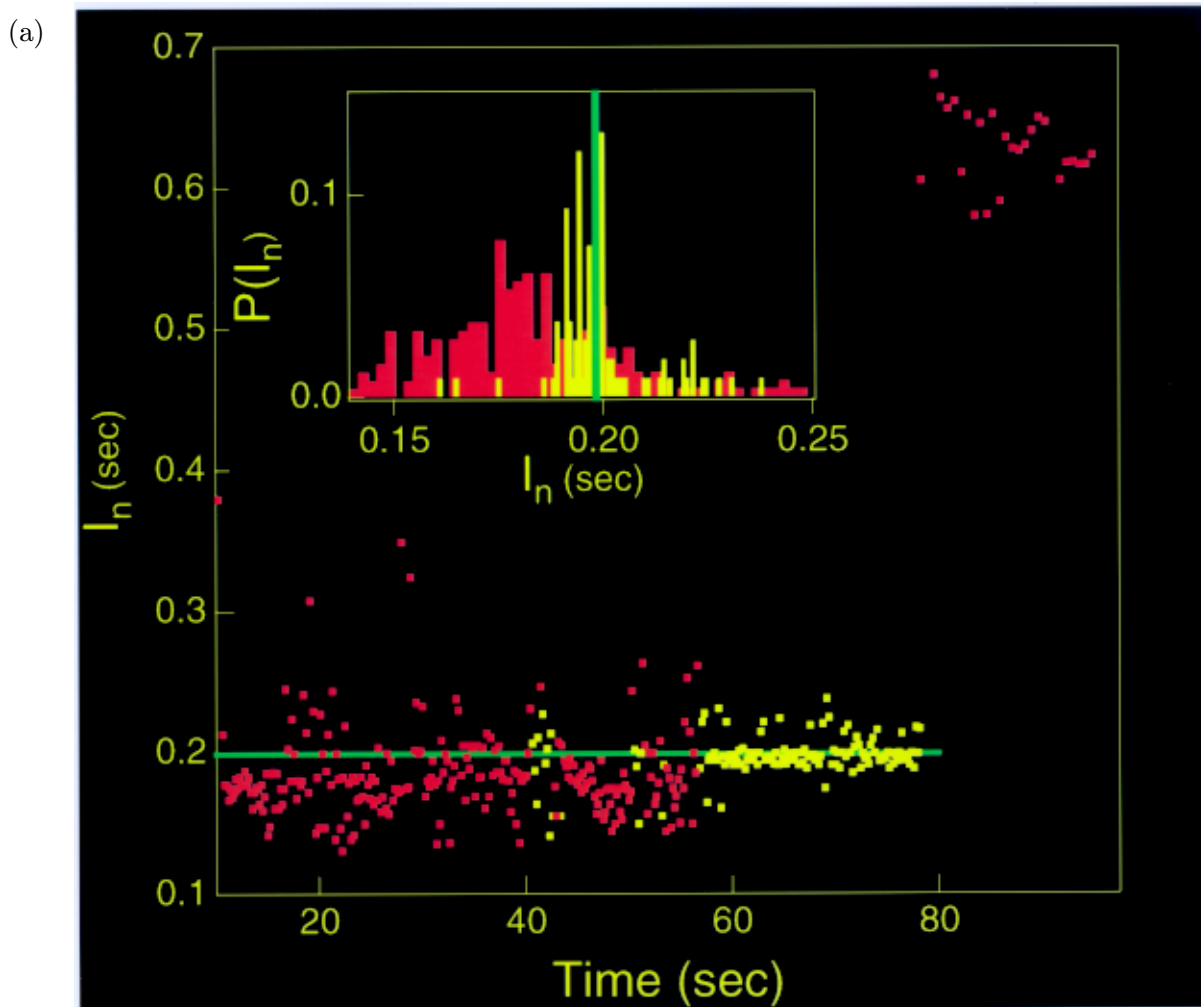


Fig. 4. (a) Interval time series before and during control. The mean of the controlled intervals was equal to or longer than the mean of the activation intervals of the spontaneous atrial fibrillation, and the standard deviation from the mean of the controlled data was at least two times less than the standard deviation from the mean of the uncontrolled activation intervals as shown in the inset. (b) Histogram of the data on a Poincaré plot before and (c) after implementation of chaos control.

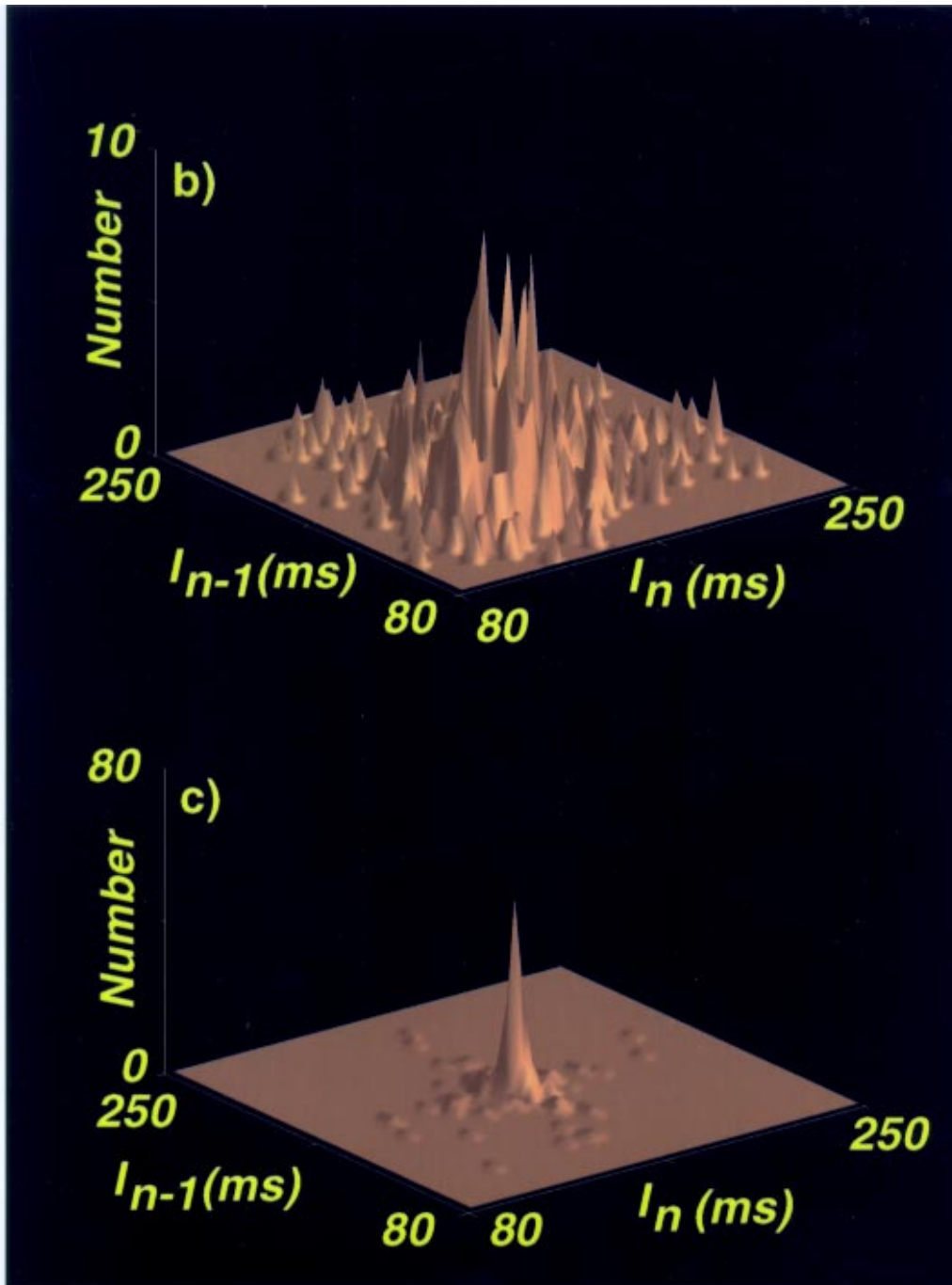


Fig. 4. (Continued)

leaving the shorter ones unchanged. In contrast, the current results demonstrate the effectiveness of chaos control for entraining the atrium at intervals equal to and significantly longer than the mean spontaneous interval with the ability to eliminate both short and long fluctuations about the mean interval. Thus it dramatically reduces the varia-

tion from the mean cycle length. Chaos control functions differently from periodic or demand pacing by locating, characterizing and exploiting the natural dynamics around a UFP in the Poincaré plot and initiating a stimulus only when the system state comes near the UFP. The stimulus forces a predicted interval onto the stable manifold (the

contracting direction) and allows the natural contraction along the stable manifold to pull the state point onto the UFP, thereby minimizing the number of control interventions needed. Chaos control is a feedback control technique and uses real-time monitoring of the Poincaré plot with constant adjustments of the control stimuli. This is important in noisy systems like the heart. It is important to note that chaos control uses control stimuli to exploit the natural contraction of the stable *direction* of a UFP rather than enforcing a rigid target *point*.

5. Summary

In conclusion, we have shown that chaos control can be used to stabilize an unstable fixed point whose corresponding activation interval was equal to or significantly longer than the mean of the uncontrolled activation intervals during human atrial fibrillation. We note that these experiments have no direct clinical implications. Indeed, our experiments were conducted while the patients were in the hospital preparing for other cardiac treatment such as ablation. The application of these other treatments immediately following our tests made long-term studies moot. The work presented here was by design limited to the study of phenomenology involved in the control schemes, with the eventual hope of designing a device that could intervene as needed in the event of fibrillation.

Several unresolved questions remain. First we are uncertain as to the spatial extent of the atrium captured during chaos control. A previous study on the regional entrainment of atrial fibrillation in dogs [Allessie *et al.*, 1991] has shown a capture region of 4 cm in diameter. We are currently working on determining the spatial extent of such chaos control in animal experiments [Witkowski *et al.*, 1998]. Second, while sinus rhythm occasionally follows chaos, further studies will be required to determine a causal connection. Third, it is an open question, in lieu of chaos control-induced cardioversion, whether chaos control can lower the energy threshold required for defibrillation of the atrium. The atrial defibrillation threshold, even with newly developed endocardial leads, remains sufficiently high to result in stimulation of skeletal muscles and patient discomfort [Wickelgren, 1996]. Despite these uncertainties, chaos control in human atrial fibrillation offers a promising alternative for altering the dynamics of the arrhythmia. This alternative requires much less energy than the existing high

energy shock techniques, which are designed to overpower the dynamics of the atrium. Thus a better understanding of the dynamics of human atrial fibrillation and its response to chaos control techniques presents us with an intriguing new direction for the study and treatment of human fibrillation.

References

- Allessie, M., Kirchhof, C., Scheffer, G. J., Chorro, F. & Brugada, J. [1991] "Regional control of atrial fibrillation by rapid pacing in conscious dogs," *Circulation* **84**, 1689–1697.
- Chialvo, D. R. [1990a] "Non-linear dynamics of cardiac excitation and impulse propagation," *Nature* **330**, 749–752.
- Chialvo, D. R., Gilmour, R. F., Jr. & Jalife, J. [1990b] "Low dimensional chaos in cardiac tissue," *Nature* **343**, 653–657.
- Christini, D. J. & Collins, J. J. [1995] "Using noise and chaos control to control nonchaotic systems," *Phys. Rev.* **E52**, p. 5806.
- Christini, D. J. & Collins, J. J. [1996] "Using chaos control and tracking to suppress a pathological nonchaotic rhythm in a cardiac model," *Phys. Rev.* **E53**, R49–R52.
- Ding, M., Yang, Y., In, V., Ditto, W. L., Spano, M. L. & Gluckman, B. [1996] "Controlling chaos in high dimensions: Theory and experiment," *Phys. Rev.* **E53**, 4334–4344.
- Ditto, W. L. & Pecora, L. M. [1993] "Mastering chaos," *Sci. Am.* **269**(2), 78–84.
- Garfinkel, A., Chen, P. S., Walter, D. O., Karagueuzian, H. S., Kogan, B., Evans, S. J., Karpoukhin, M., Hwang, C., Uchida, T., Gotoh, M., Nwasokwa, O., Sager, P. & Weiss, J. N. [1997] "Quasiperiodicity and chaos in cardiac fibrillation," *J. Clinical Investigation* **99**(2), 305–314.
- Garfinkel, A., Spano, M. L., Ditto, W. L. & Weiss, J. N. [1992] "Controlling cardiac chaos," *Science* **257**, 1230–1235.
- Hall, K., Christini, D. J., Tremblay, M., Collins, J. J., Glass, L. & Billete, J. [1997] "Dynamic control of cardiac alternans," *Phys. Rev. Lett.* **78**, 4518–4521.
- Kannel, W. B., Abbott, R. D., Savage, D. D. & McNamara, P. M. [1982] "Epidemiologic features of chronic atrial fibrillation," *New England J. Med.* **306**, 1018–1022.
- Kirchhof, C., Chorro, F., Scheffer, G. J., Brugada, J., Konings, K., Zetelaki, Z. & Allessie, M. [1993] "Regional entrainment of atrial fibrillation studied by high-resolution mapping in open-chest dogs," *Circulation* **88**, 736–749.
- Ott, E. & Spano, M. L. [May, 1995] "Controlling chaos," *Phys. Today* **48**, 34–40.

- Pei, X. & Moss, F. [1996] "Characterization of low-dimensional dynamics in the crayfish caudal photoreceptor," *Nature* **379**, 618–621.
- Petrov, V., Schatz, M. F., Muehlner, K. A., VanHook, S. J., McCormick, W. D., Swift, J. B. & Swinney, H. L. [1996] "Nonlinear control of remote unstable states in a liquid bridge convection experiment," *Phys. Rev. Lett.* **77**, 3779–3782.
- Petrov, P. & Showalter, K. [1996] "Nonlinear control of dynamical systems from time series," *Phys. Rev. Lett.* **76**, 3312–3315.
- Pierson, D. & Moss, F. [1995] "Detecting periodic unstable points in noisy chaotic and limit cycle attractors with applications to biology," *Phys. Rev. Lett.* **75**, 2124–2127.
- Prystowsky, E. N., Benson, W. J., Fuster, V., Hart, R. G., Kay, G. N., Myerburg, R. J., Naccarelli, G. V. & Wyse, G. [1996] "Management of patients with atrial fibrillation," *Circulation* **93**, 1262–1277.
- Schiff, S. J., Jerger, K., Duong, D. H., Taeun, C., Spano, M. L. & Ditto, W. L. [1994] "Controlling chaos in the brain," *Nature* **370**, 615–620.
- Shinbrot, T., Grebogi, C., Ott, E. & Yorke, J. A. [1993] "Using small perturbations to control chaos," *Nature* **363**, p. 411.
- So, P., Ott, E., Schiff, S. J., Kaplan, D. T., Sauer, T. & Grebogi, C. [1996] "Detecting unstable periodic orbits in chaotic experimental data," *Phys. Rev. Lett.* **76**, 4705–4708.
- So, P., Ott, E., Sauer, T., Gluckman, B. J., Grebogi, C. & Schiff, S. J. [1997] "Extracting unstable periodic orbits from chaotic time series data," *Phys. Rev.* **E55**, 5398–5417.
- Theiler, J., Eubank, S., Longtin, A., Galdrikian, B. & Farmer, J. D. [1992] "Testing for nonlinearity in time series: The method of surrogate data," *Physica* **D58**, 77–94.
- Wickelgren, I. [1996] "New devices are helping transform coronary care," *Science* **272**, 668–670.
- Witkowski, F. X., Kavanagh, K. M., Penkoske, P. A., Plonsey, R., Spano, M. L., Ditto, W. L. & Kaplan, D. T. [1995] "Evidence for determinism in ventricular fibrillation," *Phys. Rev. Lett.* **75**, 1230–1233.
- Witkowski, F. X., Leon, L. J., Penkoske, P. A., Giles, W. R., Spano, M. L., Ditto, W. L. & Winfree, A. T. [1998] "Spatiotemporal evolution of ventricular fibrillation," *Nature* **392**, 78–82.